Molecular Biology of the Cell
Vol. 16, 1056–1070, March 2005

A Spindle Checkpoint Functions during Mitosis in the Early *Caenorhabditis elegans* Embryo[D][V]

Sandra E. Encalada,* John Willis, Rebecca Lyczak,† and Bruce Bowerman

Institute of Molecular Biology, University of Oregon, Eugene, OR 97403

Submitted August 17, 2004; Revised November 29, 2004; Accepted December 3, 2004
Monitoring Editor: Susan Strome

During mitosis, chromosome segregation is regulated by a spindle checkpoint mechanism. This checkpoint delays anaphase until all kinetochores are captured by microtubules from both spindle poles, chromosomes congress to the metaphase plate, and the tension between kinetochores and their attached microtubules is properly sensed. Although the spindle checkpoint can be activated in many different cell types, the role of this regulatory mechanism in rapidly dividing embryonic animal cells has remained controversial. Here, using time-lapse imaging of live embryonic cells, we show that chemical or mutational disruption of the mitotic spindle in early *Caenorhabditis elegans* embryos delays progression through mitosis. By reducing the function of conserved checkpoint genes in mutant embryos with defective mitotic spindles, we show that these delays require the spindle checkpoint. In the absence of a functional checkpoint, more severe defects in chromosome segregation are observed in mutants with abnormal mitotic spindles. We also show that the conserved kinesin CeMCAK, the CENP-F-related proteins HCP-1 and HCP-2, and the core kinetochore protein CeCENP-C all are required for this checkpoint. Our analysis indicates that spindle checkpoint mechanisms are functional in the rapidly dividing cells of an early animal embryo and that this checkpoint can prevent chromosome segregation defects during mitosis.

INTRODUCTION

During mitosis, some microtubules emanating from bipolar microtubule organizing centers grow toward chromosomes and attach to specialized chromosomal regions called kinetochores (Skibbens and Hieter, 1998; Cleveland *et al*., 2003). Once captured, sister chromatids are segregated, one to each of two daughter cells. Eukaryotic cells have evolved a mechanism called the spindle checkpoint, to monitor chromosomal segregation and increase the fidelity of mitosis (reviewed in Gardner and Burke, 2000; McIntosh *et al*., 2002). Until spindle microtubules from both poles capture and align all sister chromatid pairs at a metaphase plate, the spindle checkpoint produces a delay in the onset of anaphase. If this delay is bypassed by reducing checkpoint function, anaphase starts prematurely, and daughter cells may receive unequal complements of chromosomes. Such genomic instability can result in lethality and in tumorigenesis (Hartwell and Kastan, 1994; Basu *et al*., 1999).

Originally identified and characterized in *Saccharomyces cerevisiae*, seven spindle assembly checkpoint genes (*MAD1, MAD2, MAD3, BUB1, BUB2, BUB3*, and *MPS1*) are known to function at kinetochores to inhibit anaphase onset, or to mediate mitotic exit in the presence of spindle abnormalities (Hoyt *et al*., 1991; Li and Murray, 1991). Mutations in these genes reduce or eliminate the cell cycle delays that normally occur after treatment with microtubule depolymerizing drugs (Wang and Burke, 1995; Pangilinan and Spencer, 1996). Bub1 and Bub3 form a protein kinase complex that, in concert with Mps1, functions at kinetochores upstream of Mad1 and Mad2 (Roberts *et al*., 1994; Hardwick and Murray, 1995; Hardwick *et al*., 1996). One target of the spindle checkpoint signal is the anaphase-promoting complex/cyclosome, an E3 ubiquitin ligase that targets cell cycle proteins, including the securins Pds1 and Cut2, for proteosome-mediated degradation (Hwang *et al*., 1998).

Several checkpoint proteins are widely conserved, and new components continue to be identified in other organisms (Cleveland *et al*., 2003). A Bub1-related kinase, called hBubR1 in humans and Mad3 in other organisms, binds CENP-E, a kinesin motor protein that directly tethers kinetochores and kinetochore-bound checkpoint components to spindle microtubules and also is involved in checkpoint signaling (Chan *et al*., 1998; Abrieu *et al*., 2000; Weaver *et al*., 2003). Both CENP-E and hBUB-1 can bind another human protein called CENP-F, which is cell cycle regulated and localizes to kinetochores (Liao *et al*., 1995; Zhu *et al*., 1995). CENP-F levels are increased at unaligned kinetochores during meiosis in mouse spermatocytes, leading to suggestions that CENP-F might play a role in meiotic spindle checkpoint signaling (Eaker *et al*., 2001). It is not clear, however, what role, if any, CENP-F has in mitotic checkpoint signaling.

In *Caenorhabditis elegans*, homologues of *MAD1* and *MAD2*, called *mdf-1* and *mdf-2*, are required for viability and promote the arrest of mitotically proliferating premeiotic germ cells exposed to nocodazole (Kitagawa and Rose, 1999). The MDF-2 protein localizes to centrosomes and chromosomes in early embryonic cells, but its role during mitosis in the early embryo remains unknown. Other conserved

This article was published online ahead of print in *MBC in Press* (http://www.molbiolcell.org/cgi/doi/10.1091/mbc.E04–08–0712) on December 22, 2004.

[D][V] The online version of this article contains supplemental material at *MBC Online* (http://www.molbiolcell.org).

Present addresses: *Department of Cellular and Molecular Medicine, University of California San Diego, Leichtag, LBR-411, La Jolla, CA 92093-0683; †Biology Department, Ursinus College, Collegeville, PA 19426.

Address correspondence to: Bruce Bowerman (bbowerman@molbio.uoregon.edu).

kinetochore components have also been identified in *C. elegans*. Two inner kinetochore proteins CENP-A and CENP-C act upstream of KNL-1, a novel kinetochore protein, and are all required for kinetochore assembly and chromosome segregation (Buchwitz *et al*., 1999; Oegema *et al*., 2001; Desai *et al*., 2003). CeBUB-1 and two CENP-F-related proteins called HCP-1 and HCP-2 also localize to kinetochores in one-cell embryos. HCP-1 and HCP-2 play a role in chromosome segregation (Moore *et al*., 1999), but the role of CeBUB-1 is unknown. Finally, the kinesin MCAK (CeMCAK) localizes to the outer surface of kinetochores and to centrosomes and is required for mitotic spindle midzone formation (Grill *et al*., 2001). It is not known whether CeMCAK, CeBUB-1, HCP-1, HCP-2, or CeCENP-C are required for spindle checkpoint function.

Although several proteins that localize to kinetochores in the early *C. elegans* embryo are important for chromosome segregation, it is not known whether they have roles in spindle checkpoint activity. However, a recent study has found that destabilizing microtubules increased the number of metaphase-staged cells in early *C. elegans* embryos. Furthermore, reducing the function of *mdf-2* and a Mad3-like gene called *san-1* decreased the observed frequency of metaphase stage cells after microtubule destabilization, suggesting that a spindle checkpoint functions in the early embryo (Nystul *et al*., 2003). Studies in *Drosophila* have shown that microtubule inhibitors arrest early embryos with metaphase-like chromatin (Zalokar 1976; Foe and Alberts, 1983), and abnormally compacted chromosomes delay anaphase and result in nuclear "fallout" (Sullivan *et al*., 1993). However, the failure of microtubule depolymerizing drugs such as nocodazole to arrest mitosis in early embryonic cells has led to suggestions that the rapid mitotic divisions that occur in some early embryos do not use a spindle checkpoint (Murray and Hunt, 1997). Here, we show that both chemical and mutational disruption of the microtubule cytoskeleton in the early *C. elegans* embryo result in modest but reproducible mitotic delays at the transition to anaphase. We also show that conserved spindle checkpoint genes are required for these delays. Furthermore, we provide the first evidence that two CENP-F-like proteins, HCP-1 and HCP-2, the core kinetochore component CeCENP-C, and the mitotic kinesin CeMCAK are required, directly or indirectly, for spindle checkpoint function.

MATERIALS AND METHODS

Strains and Genetic Analyses

N2 Bristol was used as the wild-type strain and maintained according to standard methods (Brenner, 1974). The following alleles listed by chromosome number were used: *apo-5(or358ts)*, *dpy-5(e61)*, I; *dnc-1(or404ts)*, *dpy-20(e1282)*, *him-8(e1489)*, *unc-8(e49)*, IV; *lin-2(e1309)*, X. The following strains carrying integrated green fluorescent protein (GFP) constructs were used to visualize centrosomes and DNA: AZ244: *unc-119(ed3)* III; ruIs57[*unc-119(+) pie-1*::GFP::tubulin]. GFP expressed in β-tubulin labels microtubules and centrosomes (Praitis *et al*., 2001); pJH4.52: his-11::GFP. GFP expressed in H2B histones throughout the cell cycle (Strome *et al*., 2001).

apo-5(or358ts) and *dnc-1(or404ts)* were isolated in a screen for temperature-sensitive (*ts*) maternal-effect embryonic-lethal mutations, using methods described previously (Encalada *et al*., 2000). Both *or358* and *or404* were backcrossed five times by using either *him-8* or N2 males. Mutant worms were maintained at the permissive temperature (15°C). L4 larvae were shifted to the restrictive temperature (26.6°C) overnight before phenotypic analysis. Homozygous *apo-5(or358ts)* hermaphrodites produce 2% dead embryos at 15°C (5/244), whereas 100% dead embryos were produced by homozygous hermaphrodite L4 larvae shifted to 26.6°C (2469/2469). Genetic analysis of *dnc-1(or404ts)* indicates that homozygous mutant hermaphrodites produce 0.4% (3/750) dead embryos at the permissive temperature of 15°C, whereas 100% (600/600) of the embryos produced at 26.6°C failed to hatch. To test for zygotic requirements, homozygous *unc-8 dnc-1(or404)* hermaphrodites were crossed to *him-8* males. Heterozygous progeny (with genotypes *unc-8 or404/+*; *him-8/+*) were singled and placed at 26.6°C. All embryos from heterozygous parents hatched, and one-quarter (100/400) of the progeny had the Unc phenotype and were fertile, suggesting no zygotic requirement for *or404ts*. Heterozygous *apo-5 dpy-5/+*; *him-8/+* produced 16% dead embryos (155/996) at 26.6°C. Approximately 15% (123/841) of the embryos that hatched were Dpy, suggesting that the dead embryos produced by heterozygous parents reflect at least in part an essential but not fully penetrant zygotic requirement for *apo-5*.

The *apo-5* mutant was mapped to linkage group (LG) III by crossing *ts* males from *him* strains and MT3751 (*dpy-5* I; *rol-6* II; *unc-32* III) hermaphrodites. Progeny of the outcrossed hermaphrodites were examined for exclusion of the *ts* mutation by a homozygous marker chromosome, which indicated linkage. To map *apo-5*, Blister nonLin and Lin nonBlister recombinant progeny were picked from an *apo-5/bli-3 lin-17* strain. Of 33 Lin nonBlister, six picked up *apo-5*, whereas eight of eight Blister nonLin picked up *apo-5*. These data position *apo-5 (or358)* at approximately −8.7 map units on LG III.

Cloning of dnc-1

or404ts was mapped to LG IV by using visible markers, following standard methods (Brenner, 1974). Unc nonDpy and Dpy nonUnc recombinant progeny were picked from an *or404ts/unc-8 dpy-20* strain. In 22/28 Unc nonDpy recombinants, *or404ts* was linked to *unc-8*, and in 2/20 Dpy nonUnc recombinants, *or404ts* was linked to *dpy-20*. These data positioned *or404ts* to approximately +4.9 map units on chromosome IV. Previous analysis revealed that reducing the function by injection of single-stranded RNA (RNA interference, RNAi) of dynactin (*dnc-1*, ZK593.5), which maps at +4.8, produced embryos with P_0 spindle defects similar to those of *or404ts* (Skop and White, 1998). Genomic DNA fragments of the gene ZK593.5 were polymerase chain reaction (PCR) amplified and sequenced from *or404ts* mutants and compared with those from *lin-2* mutants, the strain used for mutagenesis. Three separate PCR amplifications were pooled and sequenced for each of the mutant strains. The sequenced DNA included 400 base pairs upstream and downstream of the start and stop codons, for a total of 6959 base pairs. Sequencing was performed at the University of Oregon DNA Sequencing Facility using a Beckman Coulter CEQ 800 genetic analysis sequencer. Sequence analysis revealed a missense mutation in *or404ts* at nucleotide position 5730 (cgt to tgt), corresponding to amino acid 1189 (arg to cys) that was not present in either *lin-2* or the wild-type strain. To confirm the identity of *or404ts*, germline transformation of homozygous *or404* mutants was performed using cosmid ZK593. The concentration of injected cosmid was 5 ng/μl, and a dominant *rol-6* (pRF4) gene was coinjected and used as a marker for transformation, at a concentration of 50 ng/μl. Genomic yeast DNA was used as a carrier at a concentration of 50 ng/μl. Three stable transmitting lines were obtained; in all three lines the embryonic lethality of *or404ts* was complemented at the restrictive temperature.

Live Embryo Imaging

For live imaging of wild-type, *apo-5(or358)* and *dnc-1(or404)* embryos by using differential interference contrast (DIC) microscopy, gravid hermaphrodites were dissected and embryos were mounted in M9 buffer (Brenner, 1974) on 3% agarose pads, covered with a coverslip, and filmed as described previously (Encalada *et al*., 2000). To measure the duration of mitotic stages, embryos from hermaphrodites carrying GFP strains were mounted on 3% agarose pads, covered with a coverslip, and DIC and fluorescence time-lapse movies of some GFP strains were made using a spinning disk confocal microscope (PerkinElmer Life and Analytical Sciences, Boston, MA) as described in Hamill *et al*. (2002). Other fluorescence time-lapse movies were made using a Nikon Eclipse TE200-U spinning disk microscope mounted with a Hamamatsu digital camera ORCA-ER and a Wallac Ultraview confocal scanner. Z-series were taken for all movies, by using both DIC and epifluorescence (GFP) images, acquiring six focal planes at 1-μm intervals every 10 s, or seven focal planes at 1-μm intervals every 7 s. Time points measured were chromosome condensation (prophase, the first instance when chromosomes could be individually distinguished in fluorescent images), prometaphase (at the beginning of pronuclear envelope breakdown; PNEBD), metaphase, anaphase (first instance of separation of chromosomal masses), and nuclear envelope reformation (NER). PNEBD and NER were determined by analysis of DIC images, whereas the other stages were determined by analysis of fluorescent images. Images were assembled using Adobe Photoshop (version 7.0). Pairwise comparisons of mitotic timing were done using Student's *t* test statistics. We used the *t* test because this test is commonly used to compare the actual difference between two means in relation to the variation in the data (Brauchle *et al*., 2003). Student's *t* test was used for comparing the means of two treatments (with or without even number of replicates).

Nocodazole Treatment

To depolymerize microtubules in two-cell embryos, wild-type gravid hermaphrodites carrying the β-tubulin::GFP; histone2B::GFP construct were dissected in water, and embryos were placed directly on gasket poly-lysine-coated glass slides (Erie Scientific, Portsmouth, NH). One-cell embryos were observed in water by using a stereomicroscope until 4 min after the beginning of cytokinesis. The water was then removed almost entirely, and nocodazole

was immediately added at concentrations of 20, 40, 50, or 100 μg/ml. At this time, centrosomes in newly formed AB and P_1 blastomeres that have duplicated are small, and astral microtubules have disassembled from the previous (first) mitotic cell cycle. Application of nocodazole at this time prevented the reformation of astral microtubules during the second cell division. Although in earlier studies the eggshell was cracked to introduce nocodazole into the early embryo (Strome and Wood, 1983), we have found that nocodazole can effectively penetrate the early embryo eggshell without cracking, as determined by mispositioned mitotic spindles and the partial depletion of microtubules of one- and two-cell embryos (Kurz *et al*., 2002). Slides were overlaid with a 22 × 22-mm glass coverslip and sealed with melted petroleum jelly. Timing from PNEBD to NER was measured in embryos with small or undetectable mitotic spindles, by using a spinning disk microscope as outlined above. Timing of mitotic cell cycle of two-cell embryos did not significantly change with the different concentrations of nocodazole (our unpublished data).

RNA-mediated Interference

To analyze the phenotype of kinetochore or spindle assembly checkpoint genes, double-stranded RNA (dsRNA) was made in vitro and microinjected into the gonads of either wild-type or *apo-5(or358ts)* hermaphrodites, at a concentration of at least 1 mg/ml. Double-stranded RNA was made by PCR amplification from genomic N2 DNA with primers specific to each of the following genes: *Cebub-1* (R06C7.8: ctcagtcacagagtcatcaaagcct, gctgtcgttactcatcagagcatct), *hcp-1* (ZK1055.1: ccgagcatgaggagtcaatca, catgagcgatctgaactct), *hcp-2* (T06E4.1: cagtcaacatctcagcatga, acgatgtgcatcgtttagctgac), *mdf-1* (C50F4.11: tcttcgcagtttgtttggtg, cacgagcgatttctctttcc), *mdf-2* (Y69A2AR.30a: cgggagaattcgaatcttaaact, ttccttcttccaccaattagtca), *CeCENP-C* (T03F1.9: ggaaatgtacggagcgaaaa, ccttgctcgtatgcatctct), *CeMCAK* (K11D9: gtgagtcgcatccttcgagaaga, ggagaattgtgatgtcacgagaag), and *zyg-9* (F22B5.7: acttcgatgagctgcgagaatc, atctctcaacgagtgcgccatagt). Both the forward and reverse specific primers had extensions with T7 promoters that were used for the PCR amplifications with a T7 primer. PCR reactions were cleaned with phenol: chloroform and ethanol precipitated. In vitro transcription reactions containing 5× transcription buffer, 25 mM rNTPs (3.3 mM final concentration), 0.3% RNAsin, 10% dithiothreitol, water, T7 RNA polymerase, and the PCR product were incubated at 37°C for 2 h. Transcription reactions were subsequently cleaned by phenol:chloroform and ethanol precipitated. Pellet was eluted with 30–40 μl of deionized water and kept at –20°C. *wrm-1* dsRNA was made from a cDNA clone (yk213d6; provided by Yuji Kohara, National Institute of Genetics, Nishima, Japan). Single-stranded RNA (ssRNA) from *dhc-1* (T12E12.4) was made following the same protocols described above and using the following primers: aaggaaggagctcaacgaca, ctttccttcctgggtcttc. Adult hermaphrodites were injected with *dhc-1* ssRNA at a concentration of 1 mg/ml. Worms injected with RNA were placed overnight at 26.6°C for next-day analysis. Hermaphrodites injected with *dhc-1* ssRNA produced 36% (41/156) dead embryos 0–16.5 h postinjection and 100% (83/83) dead embryos 16.5–38.5 h postinjection. Adult hermaphrodites injected with *hcp-1* and *hcp-2* dsRNA produced 74/79 (94%) dead embryos ~20–35 h postinjection at 26.6°C. Hermaphrodites injected with *mdf-1* and *mdf-2* dsRNA produced 6% (8/126) and 3% (7/238) dead embryos, respectively, 17–26 h postinjection, consistent with results from previous studies (Kitagawa and Rose, 1999). Hermaphrodites injected with *Cebub-1* dsRNA, produced 99% (673/678) dead embryos 12.5–41 h postinjection, and those injected with *CeMCAK* dsRNA produced 92% (122/132) 17–27.5 h postinjection.

Immunocytochemistry

Homozygous mutant *apo-5(or358)* and *dnc-1(or404)* hermaphrodites and hermaphrodites injected with *Cebub-1* and *CeMCAK* dsRNA were placed at 26.6°C overnight (17–20 h), and their embryos were fixed and stained the next day with an antibody against α-tubulin (DMIα; Sigma-Aldrich, St. Louis, MO). Hermaphrodites injected with *hcp-1/2*, *CeMCAK*, and *Cebub-1* dsRNA were placed at 26.6°C overnight (17–20 h), and their embryos were fixed and stained with anti-CeBUB-1, CeMCAK (provided by Karen Oegema, Ludwig Institute for Cancer Research, University of California San Diego, La Jolla, CA), and HCP-1 antibodies (provided by Mark Roth, Fred Hutchinson Cancer Research Center, University of Washington, Seattle, WA), following previously described protocols (Moore *et al*., 1999; Oegema *et al*., 2001). Imaging of stained embryos was done on a Bio-Rad 2100 Radiance confocal microscope, by using a 60× oil immersion lens. Confocal images were assembled into figures using Adobe Photoshop (version 7.0).

RESULTS

A Functional Spindle Checkpoint in the Early C. elegans Embryo

Microtubule instability can delay, and in some cases arrest, mitosis in many organisms. We examined this response in *C. elegans*, by using nocodazole to destabilize microtubules in two-cell stage embryos (see *Materials and Methods*). In earlier studies, nocodazole was shown to largely, although not entirely, deplete spindle microtubules in dividing one-cell stage *C. elegans* embryos, without arresting mitosis (Strome and Wood, 1983; Hyman and White, 1987). Exposing one-cell embryos to nocodazole produced variable effects (our unpublished data), possibly due to variability in the post-fertilization age of one-cell embryos dissected from adults when exposed to this chemical. We therefore chose instead to expose early two-cell stage embryos to nocodazole, 4 min after the initiation of the cytokinetic furrow in dividing one-cell stage embryos (see *Materials and Methods*), normalizing embryos with respect to exposure time during the cell cycle. At this early time of exposure, the newly duplicated centrosomes in both the recently formed anterior (AB) and posterior (P_1) daughters are small, with few astral microtubules. Exposure to nocodazole largely prevented reformation of astral microtubules later in the cell cycle (our unpublished data). We timed mitotic progression in untreated and nocodazole-treated early embryos from transgenic mothers that maternally express both β-tubulin::GFP and histone2B::GFP fusion proteins to label microtubules and chromosomes, respectively (Praitis *et al*., 2001; Strome *et al*., 2001). We made time-lapse movies of these embryos by using both DIC and epifluorescence optics, with a spinning disk confocal microscope (see *Materials and Methods*). Because chromosomes never formed metaphase plates and anaphase was abnormal in nocodazole-treated embryos, we

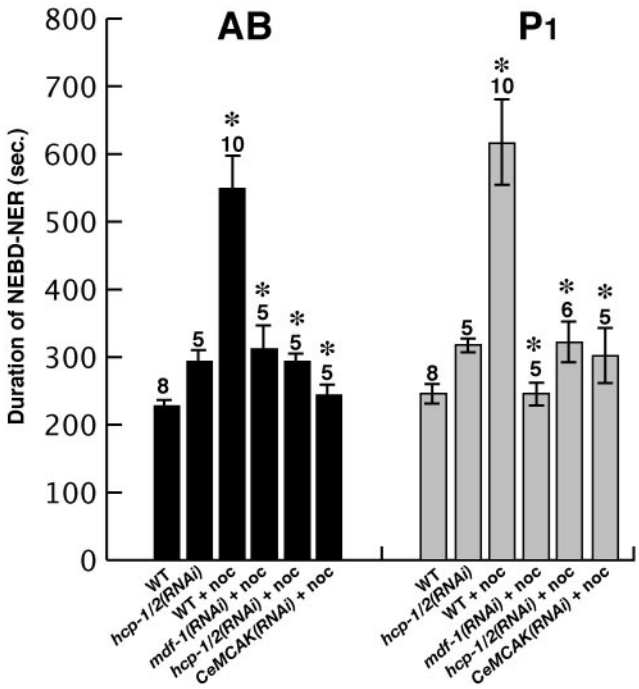

Figure 1. Depletion of MDF-1, HCP-1/2, or CeMCAK restores normal mitotic timing in two-cell stage *C. elegans* embryos exposed to nocodazole. Timing of mitosis was measured from NEBD to NER. Mean durations in seconds are plotted with SEM error bars. Numbers above bars indicate sample number for each experiment. Asterisks denote significant differences as determined by Student's *t* test statistics for comparisons between nocodazole-treated and untreated wild-type embryos and between nocodazole-treated embryos depleted from MDF-1, HCP-1/2, and CeMCAK function and nocodazole-treated wild-type embryos. Nocodazole concentrations used are as follows: WT+noc, 20, 40, 50, and 100 μg/ml; *mdf-1(RNAi)*+noc, 100 μg/ml; and *hcp-1/2(RNAi)*+noc and *CeMCAK(RNAi)*+noc, 50 μg/ml.

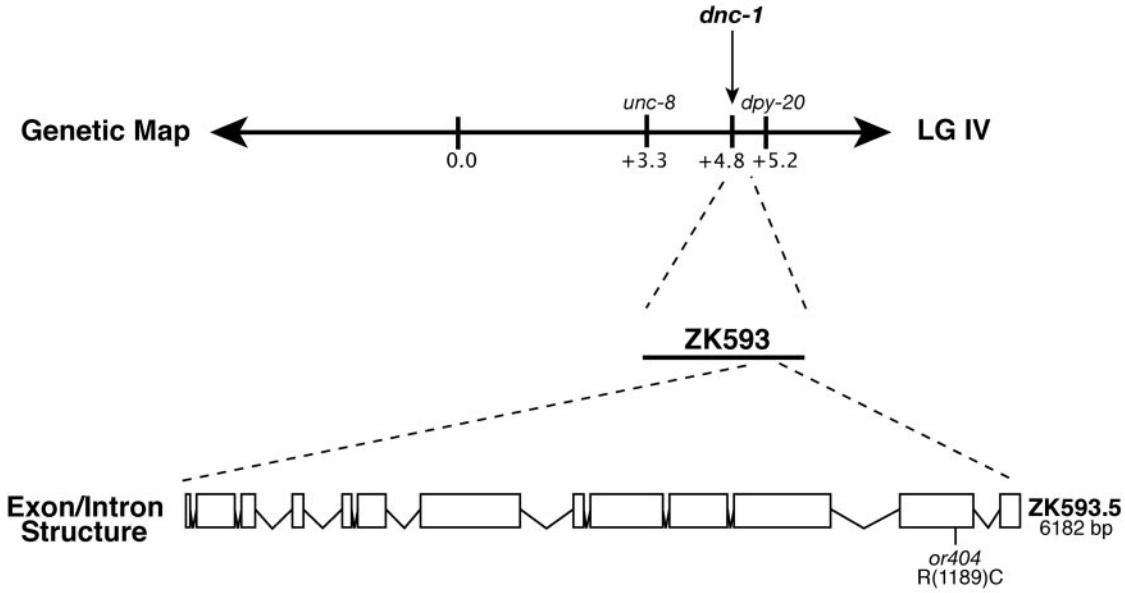

Figure 2. Molecular cloning of *dnc-1*. *dnc-1* maps approximately +4.8 map units, on LGIV (left of *dpy-20*). *dnc-1* mutants were rescued by cosmid ZK593. A single allele of *dnc-1* has a lesion in the predicted gene ZK593.5, as shown below exon 12. We identified *dnc-1(or404ts)* in a temperature-sensitive screen for embryonic lethal mutants described in Encalada *et al*. (2000).

timed mitosis from NEBD to NER by using DIC. In both the AB and P_1 cells, the duration of this interval increased 2.5-fold compared with untreated wild-type embryos (n = 10; Figure 1 and Supplementary Table 1).

If these mitotic delays are due to the activity of a spindle checkpoint, then reducing the function of checkpoint genes should restore more normal cell division timing in nocodazole-treated embryos. We therefore used RNAi to reduce the function of MDF-1, a *C. elegans* ortholog of the yeast spindle checkpoint protein Mad1p, in nocodazole-treated embryos. We found that the duration of mitosis was restored to the shorter time observed in untreated wild-type embryos (Figure 1 and Supplementary Table 1). We conclude that nocodazole-induced destabilization of microtubules in *C. elegans* embryos activates the spindle checkpoint to delay progression through mitosis.

Mitotic Delays in Mutant Embryos with Defective Spindles

As a further test of whether microtubule defects can prolong mitosis, we examined mitotic progression in mutant embryos with spindle defects in early embryonic cells, by using both Nomarski DIC and epifluorescence optics, and transgenic strains expressing β-tubulin::GFP and histone2B::GFP fusion proteins (see *Materials and Methods*). For these and all subsequent analyses of mutant embryos, we examined cell cycle progression during the first mitotic division of the zygote, when spindle defects first occur, in contrast to our use of two-cell stage embryos for nocodazole exposure.

We first timed cell cycle progression in *dnc-1(or404)* mutant embryos. The *dnc-1* gene encodes a p150Glued dynactin subunit family member and is required for proper assembly and positioning of the mitotic spindle in early embryonic cells (Skop and White, 1998; Gonczy *et al*., 1999). We identified *dnc-1(or404)* in a genetic screen for temperature-sensitive embryonic-lethal mutants with cell division defects in early embryonic cells (Figure 2). We examined embryos produced by self-fertilization in homozygous *dnc-1(or404)* mutant hermaphrodites that were matured to adulthood at the restrictive temperature of 26.6°C (hereafter referred to as mutant embryos). Using time-lapse DIC microscopy to examine the first mitotic division in *dnc-1(or404)* mutant embryos, we found that pronuclei always met and a small posteriorly displaced spindle formed (Figure 4A; n = 12). This mutant phenotype resembles the relatively weak phenotype observed after partial depletion of *dnc-1* by using RNAi, with more extensive RNAi depletion causing defects in pronuclear migration and more severe defects in spindle assembly (Skop and White, 1998; Gonczy *et al*., 1999). We conclude that *dnc-1(or404)* is a recessive, partial loss-of-function mutation. In addition to the spindle positioning and assembly defects, we also found that the average time required to progress from chromosome condensation to NER in *dnc-1* mutant embryos was increased by 1.3-fold, compared with wild-type. Similarly, the time required to progress from the breakdown of the oocyte and sperm derived pronuclei (PNEBD, which corresponds to prometaphase) to anaphase onset was increased almost twofold, compared with wild type (Figure 3A and Table 1).

Although the mitotic delay in *dnc-1* mutant embryos is consistent with activation of the spindle checkpoint, dynein has been implicated in nuclear envelope breakdown, and a reduction of dynein function can delay the onset of NEB in normal rat kidney cells (Salina *et al*., 2002). Because this delay occurs before the prometaphase-to-anaphase stage, when spindle checkpoint activity is functional, the delay in cell cycle progression we observe in *dnc-1* mutant embryos likely reflects activation of a spindle checkpoint rather than a defect in dynein function during NEB.

We next used RNAi to examine embryos depleted of either ZYG-9, a XMAP215 homolog required for microtubule stability during mitosis (Matthews *et al*., 1998), or DHC-1, the heavy chain of cytoplasmic dynein, a microtubule minus-end directed motor that, like dynactin, is required for mitotic spindle assembly (Sweeney and Holzbaur, 1996; Skop and White, 1998; Gonczy *et al*., 1999). In one-cell

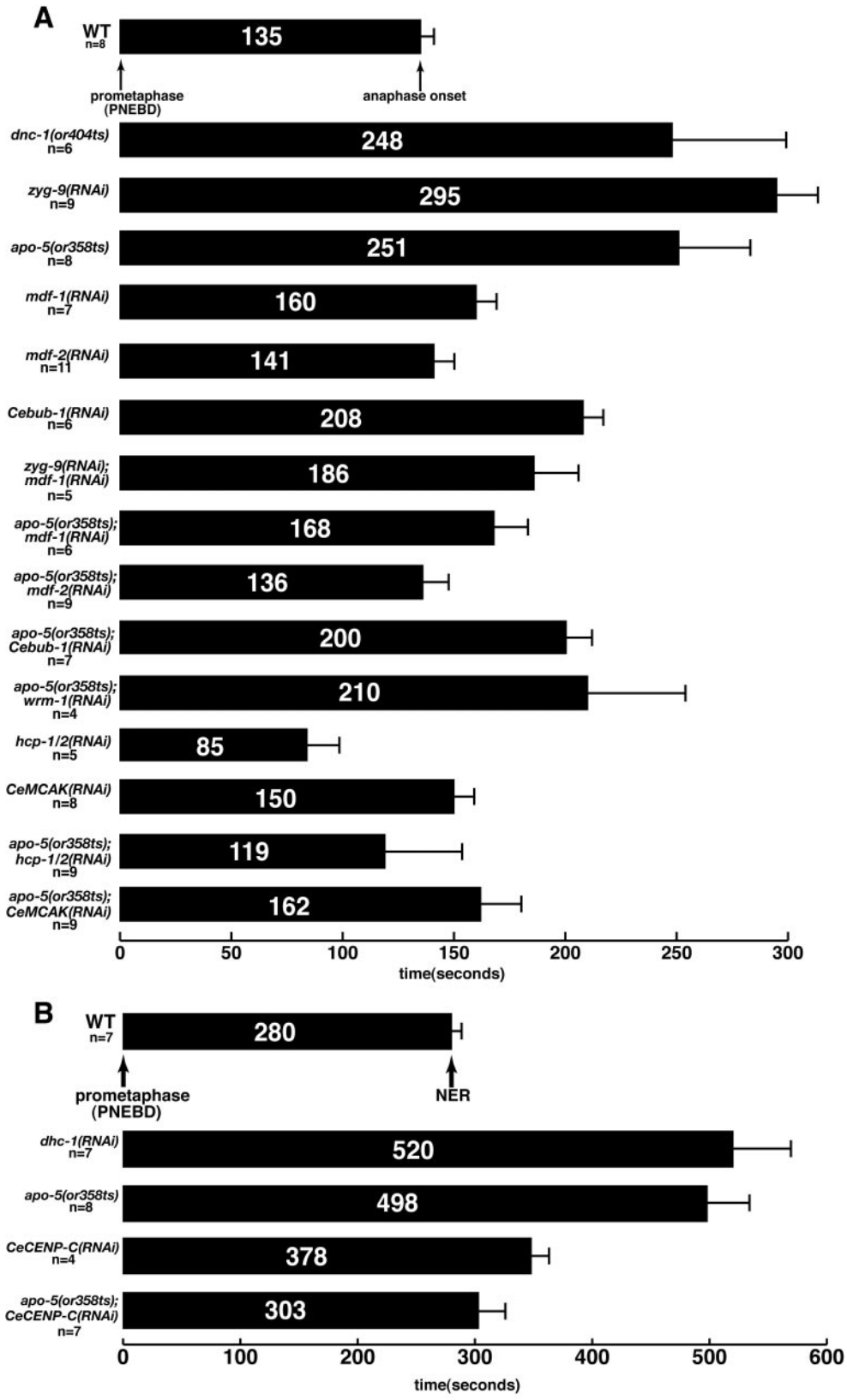

Figure 3. Depletion of spindle checkpoint proteins restores normal mitotic timing in one-cell mutant embryos with cytoskeletal abnormalities and delayed mitoses. Bars represent the duration of mitosis from prometaphase (PNEBD) to the onset of anaphase (A) or PNEBD to NER (B), in one-cell embryos. Numbers inside boxes indicate the duration of each mitotic stage in seconds. Mean durations are plotted with SEM error bars. Table 2 shows Student's *t* test statistical comparisons of mitotic timing between wild-type and mutant embryos. The p values for mitotic timing comparisons between *apo-5* and the following double mutants at the $p \leq 0.05$ level are shown in parentheses: *apo-5; mdf-1*(0.042); *apo-5; mdf-2* (0.0082); *apo-5; Cebub-1* (0.17); *apo-5; wrm-1* (0.47); *apo-5; hcp-1/2* (0.013); *apo-5; CeMCAK* (0.032); and *apo-5; CeCENP-C* (0.00067).

stage *zyg-9(RNAi)* mutant embryos, as expected, astral microtubules were abnormally short and the first mitotic spindle was mispositioned (our unpublished data). The duration of mitosis in *zyg-9(RNAi)* embryos, from chromosome condensation to NER, was ~1.5-fold longer than in wild type (Tables 1 and 2). This increase was largely due to a 2.2-fold

Table 1. Duration of mitosis in one-cell embryos

Embryo	Total mitosis[a] (s) ± SE (n)	PNEBD-anaphase (s) ± SE (n)	PNEBD-NER[b] (s) ± SE (n)
Wild type	737.1 ± 32.7 (7)	135.0 ± 6.0 (8)	280.0 ± 8.5 (7)
dnc-1(or404)	933.3 ± 288.7 (3)	248.3 ± 51.0 (6)	
zyg-9(RNAi)	1106.7 ± 79.6 (6)	294.5 ± 18.3 (9)	
apo-5(or358)	1010.0 ± 100.3 (7)	251.3 ± 32.1 (8)	497.5 ± 35.7 (8)
mdf-1(RNAi)	865.0 ± 27.5 (5)	160.0 ± 9.0 (7)	
mdf-2(RNAi)	683.3 ± 84.1 (3)	140.9 ± 8.8 (11)	
Cebub-1(RNAi)	946.6 ± 35.3 (3)	208.3 ± 8.7 (6)	
zyg-9(RNAi); mdf-1(RNAi)	na	186.0 ± 19.9 (5)	
apo-5(or358); mdf-1(RNAi)	866.0 ± 78.5 (5)	168.3 ± 14.9 (6)	
apo-5(or358); mdf-2(RNAi)	804.0 ± 55.6 (5)	135.6 ± 11.4 (9)	
apo-5(or358); Cebub-1(RNAi)	920.0 ± 101.2 (4)	200.0 ± 11.3 (7)	
apo-5(or358); wrm-1(RNAi)	na	210.0 ± 43.8 (4)	
hcp-1/2(RNAi)	805.0 ± 33.3 (4)	84.0 ± 14.4 (5)	
CeMCAK(RNAi)	825.7 ± 73.4 (7)	150.0 ± 8.9 (8)	
apo-5(or358); hcp1/2(RNAi)	1210.0 ± 171.0 (3)	118.9 ± 34.5 (8)	
apo-5(or358); CeMCAK(RNAi)	na	161.7 ± 17.8 (12)	
dhc-1(RNAi)	1350.0 ± 234.3 (3)	na	520.0 ± 49.7 (7)
CeCENP-C(RNAi)	na	na	347.5 ± 14.9 (4)
apo-5(or358); CeCENP-C(RNAi)	842.0 ± 55.8 (5)	na	302.9 ± 22.8 (7)

na, not available.

[a] Duration of timing from chromosome condensation (beginning of prophase) to NER.

[b] Duration of timing from PNEBD to NER was measured for wild-type, *apo-5* embryos and for embryos in which clear segregation of chromosomes (anaphase) was not obvious.

lengthening of the interval from prometaphase to anaphase (Figure 3A and Table 1). In *dhc-1(RNAi)* embryos, severe spindle assembly defects preclude the use of metaphase and anaphase as landmarks (Skop and White, 1998; Gonczy *et al*., 1999). We therefore assessed the duration of mitosis by measuring the time from PNEBD to NER in one-cell *dhc-1(RNAi)* embryos by using DIC optics. Progression through this interval took almost twice as long compared with wild type (Figure 3B and Tables 1 and 2).

Finally, we examined cell cycle progression in *apo-5(or358)* mutant embryos. We identified *apo-5(or358)* in our screens for conditional embryonic-lethal mutants but have not yet determined its molecular identity (see *Materials and Methods*). Using time-lapse Nomarski DIC movies, we found that in most *apo-5* mutant embryos (27/28), the position of the first mitotic spindle was unstable, often residing abnormally near the posterior pole during anaphase (Figure 4, A and B). We therefore chose the name *apo-5* for *a*naphase spindle *po*sition-defective. We also used indirect immunofluorescence with an antibody that recognizes α-tubulin to examine microtubules in fixed one-cell stage *apo-5(or358)* and wild-type embryos. Compared with wild-type embryos (n = 12), mitotic astral microtubules were short in *apo-5* mutants at metaphase (3/3) and anaphase (7/8), and short microtubule fragments were detected throughout the cytoplasm (Figure 4C). Analyses of one-cell *apo-5* embryos containing β-tubulin::GFP and histone2B::GFP fusion constructs revealed that chromosomes do not align normally during metaphase and anaphase, presumably due to defects in kinetochore–microtubule attachment or stability (see Supplemental Movies). As in the other spindle defective mutants, we found that the time required to progress from chromosome condensation to NER was 1.4-fold longer in *apo-5* mutant embryos, compared with wild type (Table 1). Nearly twofold delays occurred during the interval from PNEBD to anaphase (Figure 3 and Table 1). To summarize, we have found that mitotic spindle defects in *dnc-1*, *zyg-9*, *dhc-1*, and *apo-5* mutant embryos are associated with modest but reproducible delays in progression through mitosis.

A Spindle Checkpoint Delays Mitosis and Reduces Chromosome Segregation Defects in Embryonic Cells with Abnormal Mitotic Spindles

To determine whether the mitotic delays in spindle-defective mutant embryonic cells require a spindle checkpoint, we used RNAi to reduce the function of MDF-1, MDF-2, and CeBUB-1, *C. elegans* orthologues of the yeast spindle check-

Table 2. Student's *t* test statistics for pairwise comparisons of duration of mitosis

	mdf-1 (RNAi)[a]	*mdf-2 (RNAi*[a]	*Cebub-1 (RNAi)*[a]	*apo-5 (or358ts)*[a]	*dnc-1 (or404ts)*[a]	*zyg-9 (RNAi)*[a]	*dhc-1 (RNAi)*[b]	*hcp-1/2 (RNAi)*[a]	*CeMCAK (RNAi)*[a]	*CeCENP-C (RNAi)*[b]
Wild type	0.042*	0.59	5.7×10^{-5}*	0.0082*	0.077	0.0049*	0.0027*	0.020*	0.19	0.011*

Numbers represent p values between each pairwise comparison. Asterisks denote significant differences at the $p \leq 0.05$ level.

[a] p values were calculated for comparisons of timing from PNEBD to anaphase onset.

[b] p values were calculated for comparisons of timing from PNEBD to NER.

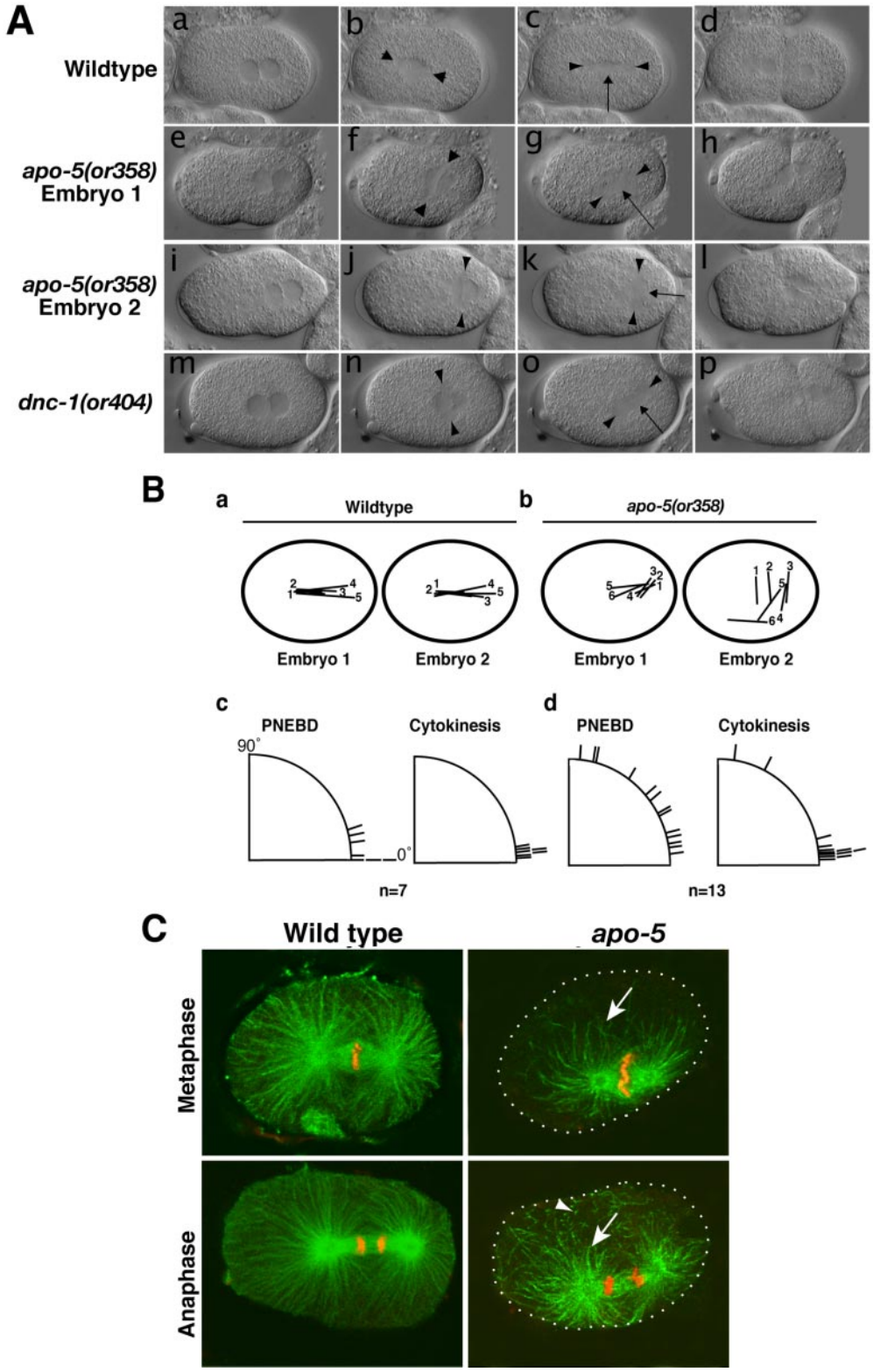

Figure 4. Microtubule cytoskeletal defects in *apo-5* and *dnc-1* mutant embryos. (A) Time-lapse Nomarski photomicrographs of a dividing wild-type one-cell stage embryo (a–d), and of two *apo-5* (e–l), and one *dnc-1* (m–p) mutant embryos undergoing their first mitotic division. Embryos are shown with anterior to the left and posterior to the right. Clearings in a, e, i, and m are the maternal and paternal pronuclei. Arrowheads point to centrosomes and arrows point to the middle of spindles. Notice short distance between nuclei in the newly formed two-cell *apo-5* and *dnc-1* embryos (h, l, and p), likely due to chromosome segregation defects. (B) Positioning and orientation of the first mitotic spindle in two wild-type (a and c) and two *apo-5* (b and d) embryos. Lines inside embryos in a and b represent the position and length of the spindle during elongation. Numbers indicate the sequential order of movement of the mitotic spindle throughout mitosis, starting at pronuclear envelope breakdown (1) and ending at cytokinesis (5 or 6). The length of the spindle was drawn at 10-s intervals. Marks on quadrants on c and d represent the angle between centrosomes and the a-p axis (0°) at PNEBD and cytokinesis. Each mark represents a single scored spindle. (C) Laser scanning confocal images of α-tubulin (green) and DNA (TOTO, red) staining of one-cell stage wild-type and *apo-5* embryos during metaphase and anaphase. Arrows point at short microtubules that do not reach the cortex of the embryo and arrowhead points to cytoplasmic tubulin fragments. Dots delineate the embryo cortex in *apo-5* mutants.

point proteins Mad1p, Mad2p, and Bub1p. We reduced the function of MDF-1, MDF-2, and CeBUB-1 in *apo-5* embryos and that of MDF-1 in *zyg-9(RNAi)* embryos. We found that reducing the function of MDF-1 decreased the mitotic delays observed in *apo-5* and *zyg-9* embryos, and reducing the function of MDF-2 restored normal timing to the first mitotic cell cycle of *apo-5* embryos (Figure 3A). *Cebub-1(RNAi)* was less effective in rescuing the mitotic delays in *apo-5* mutants, probably due to mitotic delays observed in wild-type embryos depleted of CeBUB-1 using RNAi (Figure 3A). As a negative control, we used RNAi to reduce the function of WRM-1, a β-catenin homolog not expected to influence

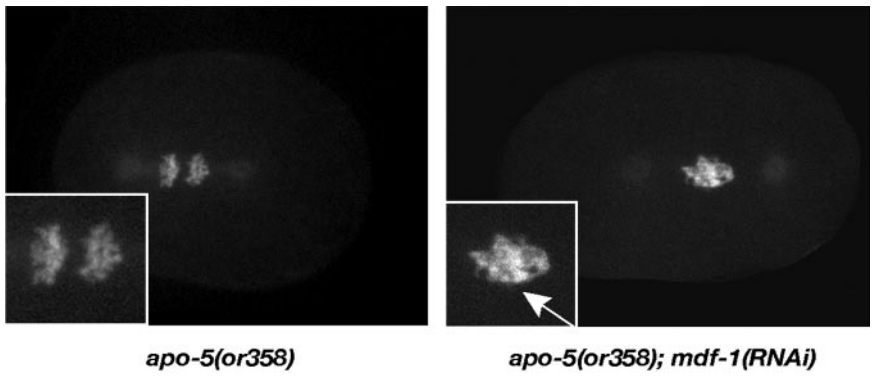

Figure 5. Increased presence of DNA bridges after disruption of MDF-1 function. Fluorescent spinning disk confocal images of one-cell stage *apo-5* and *apo-5; mdf-1* embryos showing histone2B::GFP signal. Insets show enlarged chromosomes. Arrow points to DNA bridges present in the double mutant.

checkpoint function, and we did not observe significant changes in the timing of mitosis in *apo-5* embryos (Figure 3A). We conclude that a functional spindle checkpoint monitors proper spindle assembly during early embryonic cell divisions.

To address the potential biological significance of the spindle checkpoint in early *C. elegans* embryos, we compared the frequency of DNA segregation defects in *apo-5* mutants with or without RNAi-mediated depletion of MDF-1 and MDF-2. Using time-lapse movies of one-cell embryos carrying a histone2B::GFP fusion, we observed lagging chromosomes in fewer than one-half of the dividing one-cell stage *apo-5* embryos (Figure 5 and Table 3; see Supplemental Movies). Reducing MDF-1 and MDF-2 function in *apo-5* mutants resulted in detectable chromosome segregation defects (lagging chromosomes and chromosome bridges) in nearly all embryos (Figure 5 and Table 3; see Supplemental Movies). We conclude that the spindle checkpoint can delay progression through mitosis and reduce the likelihood of chromosome segregation defects in embryonic cells with abnormal spindles.

CeCENP-C, CeMCAK, and the Two CENP-F–like Proteins HCP-1 and HCP-2 Are Required for a Functional Spindle Checkpoint

Having established that a checkpoint delays mitosis in embryonic cells with defective spindles, we asked whether other known kinetochore proteins in *C. elegans* are required for a functional spindle checkpoint. Recently, two *C. elegans* proteins called HCP-1 and HCP-2, with limited homology to mammalian CENP-F, were shown to contribute redundantly to the proper segregation of chromosomes during embryogenesis (Moore *et al*., 1999). Intriguingly, mammalian CENP-F was recently implicated in meiotic spindle checkpoint function (Eaker *et al*., 2001). The conserved kinesin CeMCAK localizes to kinetochores in *C. elegans* embryos and is required for assembly of the mitotic spindle midzone (Grill *et al*., 2001). The localization of both HCP-1 and CeMCAK to kinetochores requires a core kinetochore protein called CeCENP-C (Moore and Roth, 2001; Oegema *et al*., 2001). To better define the requirements for a functional mitotic checkpoint, we asked whether HCP-1, HCP-2, CeMCAK, and CeCENP-C are required for the mitotic delays observed in embryonic cells with defective spindles.

To examine the role of HCP-1 and HCP-2 in early embryos, we used RNAi to reduce the function of both proteins simultaneously. Reducing the function of either HCP-1 or HCP-2 alone by RNAi does not result in significant embryonic lethality, but depletion of both proteins simultaneously [hereafter referred to as *hcp-1/2(RNAi)*], has been shown to result in 99% embryonic lethality, and in embryonic cells with abnormal amounts of chromosomal DNA, presumably due to chromosome segregation defects (Moore *et al*., 1999). We also found that depletion of both HCP-1 and HCP-2 resulted in a highly penetrant embryonic lethality (see *Materials and Methods*), and we examined the chromosome segregation defects during the first mitotic division of mutant embryos by using time-lapse microscopy (see next section). Because chromosomes in one-cell stage *hcp-1/2(RNAi)* embryos did not congress to form a metaphase plate, but did move toward opposite poles (see next section), we measured the time from pronuclear envelope breakdown to the anaphase-like movements of chromosomal masses to opposite poles. The duration of this interval was shorter in *hcp-1/2(RNAi)* embryos, compared with wild-type (Figure 3A and Table 1). We next used RNAi to deplete HCP-1/2 in one-cell stage *apo-5(or358)* mutant embryos (Figure 3A) and in two-cell stage wild-type embryos treated with nocodazole (Figure 1). We found that reducing HCP-1/2 restored normal mitotic timing to *apo-5* and nocodazole-treated embryos. We also used RNAi to deplete CeMCAK function in one-cell *apo-5(or358)* mutant embryos (Figure 3A), and in nocodazole-treated two-cell stage wild-type embryos (Figure 1). In both cases, CeMCAK depletion restored a more normal timing of mitotic progression.

Finally, we examined mitotic progression in CeCENP-C–depleted embryos. As shown previously (Oegema *et al*., 2001), chromosomes do not separate in anaphase movements in one-cell *CeCENP-C(RNAi)* embryos. We thus measured mitosis in *CeCENP-C(RNAi)* embryos from PNEBD to NER and found that the timing of mitosis was similar to that of wild-type embryos. Reducing the function of CeCENP-C by RNAi in one-cell *apo-5(or358)* embryos restored nearly

Table 3. Frequency of lagging chromosomes in one-cell *C. elegans* embryos

Embryo	No. of embryos with lagging chromosomes (%)
WT	0/18 (0)
apo-5(or358ts)	10/18 (56)
mdf-1(RNAi)	1/17 (6)
mdf-2(RNAi)	1/11 (9)
apo-5(or358ts); mdf-1(RNAi)	15/16 (94)
apo-5(or358ts); mdf-2(RNAi)	8/10 (80)

WT, wild type.

normal mitotic timing, compared with wild-type (Figure 3B and Table 1). We conclude that in addition to known checkpoint proteins, the kinetochore proteins HCP-1/2, CeMCAK, and CeCENP-C also are required for a functional mitotic spindle checkpoint.

Different Requirements for HCP-1/2 and CeMCAK in Spindle Midzone Assembly and Function

Depletion of the core kinetochore protein CENP-C seems to completely disrupt kinetochore assembly (Oegema *et al*., 2001), presumably accounting for the inactivity of the spindle checkpoint in CENP-C–depleted embryos. To address how the depletion of HCP-1/2 and CeMCAK might influence the spindle checkpoint function, and to assess whether these proteins act in shared pathways, we compared the mutant phenotypes of dividing one-cell stage embryos produced after RNAi depletion of HCP-1/2, CeMCAK, and CeBUB-1, a presumed checkpoint protein.

We first examined the structure of the mitotic spindle in fixed one-cell embryos, by using indirect immunofluorescence to detect microtubules (Figure 6A). As reported by others (Grill *et al*., 2001), we found that the spindle midzone was not detectable in CeMCAK-depleted embryos (7/8 embryos; Figure 6A). The spindle midzone also was absent in *hcp-1/2(RNAi)* embryos (9/10), but it was normal in *Cebub-1(RNAi)* embryos (8/8; Figure 6A). Surprisingly, cytokinesis seemed normal during the first mitotic division in embryos from all three genotypes, despite the absence of a central spindle (our unpublished data). This is in contrast to previous studies which showed that cytokinesis always fails in the absence of a central spindle after depletion of ZEN-4, an MKLP1-like kinesin-related protein (Raich *et al*., 1998).

We next analyzed the dynamics of spindle pole separation during the first mitotic division in wild-type, *hcp-1/2(RNAi)*, *CeMCAK(RNAi)*, and *Cebub-1(RNAi)* embryos (Figure 6B). The first mitotic spindles seemed normal at pronuclear envelope breakdown in *hcp-1/2(RNAi)*, *CeMCAK(RNAi)*, and *Cebub-1(RNAi)* embryos (Figure 6B, a, g, m, and s), but by the time chromosomes had formed a metaphase plate in wild-type embryos, chromosomes in *hcp-1/2(RNAi)* or *Cebub-1(RNAi)* embryos had not properly aligned to form a metaphase plate (Figure 6B, b, h, and t). Subsequently in *hcp-1/2(RNAi)* and *CeMCAK(RNAi)* embryos, the centrosomes and chromosomes rapidly moved toward opposite poles (Figure 6B, h–l, n–r). In contrast to the abrupt centrosome separation observed in *hcp-1/2(RNAi)* embryos, centrosomes separated more gradually and to more variable extents in *CeMCAK(RNAi)* embryos. The mitotic spindle in one-cell *Cebub-1(RNAi)* embryos elongated with nearly wild-type kinetics (Figure 6B, s–x; our unpublished data). Nevertheless, mitosis was clearly abnormal in *Cebub-1(RNAi)*, progressing more slowly than in wild-type (Figures 3A) and with lagging chromosomes during anaphase (our unpublished data).

Finally, we analyzed the dynamics of spindle separation in *hcp-1/2(RNAi)*, *CeMCAK(RNAi)*, and *Cebub-1(RNAi)* embryos (Figure 6, C and D). Although centrosomes in dividing one-cell stage wild-type embryos moved apart gradually, with a slight increase in velocity during anaphase (Figure 6C, arrow), centrosomes separated abruptly in *hcp-1/2(RNAi)* embryos (Figure 6, B and C). These anaphase-like movements of chromosomes and centrosomes occurred ~85 s after PNEBD in *hcp-1/2(RNAi)* embryos, compared with 135 s in wild type, suggesting that the mutant embryos entered anaphase precociously. In agreement with previous observations (Grill *et al*., 2001), we found that centrosomes often moved abnormally far apart from each other during the first division in *CeMCAK(RNAi)* embryos (4/10 embryos; Figure 6D). Despite the premature and abnormally rapid anaphase movements in *hcp-1/2(RNAi)* and *CeMCAK(RNAi)* embryos, cytokinesis occurred at approximately the same time as in wild type (Figure 6B; our unpublished data).

In summary, depletion of CeMCAK or HCP-1/2 resulted in similar mutant phenotypes, including the absence of a central spindle and the abnormal poleward movement of centrosomes during anaphase. In contrast, depletion of CeBUB-1 does not obviously influence central spindle structure or the movement of centrosomes during anaphase. Thus, HCP-1/2 and CeMCAK may act in similar spindle midzone assembly pathways and clearly differ in their requirements compared with a known checkpoint protein, CeBUB-1.

CeBUB-1 and CeMCAK Are Required for the Localization of HCP-1 to Kinetochores

To further compare the requirements for HCP-1/2, CeMCAK, and CeBUB-1, we examined their assembly onto kinetochores in wild-type and mutant embryos. Previous studies have shown that the localization to kinetochores of HCP-1, CeMCAK, and CeBUB-1 all require two core kinetochore components, CeCENP-A (HCP-3) and CeCENP-C (HCP-4) (Moore and Roth, 2001; Oegema *et al*., 2001; Desai *et al*., 2003). CeMCAK and CeBUB-1 localize independently of each other (Oegema *et al*., 2001), but it is not known whether HCP-1/2 localization to kinetochores depends on either CeMCAK or CeBUB-1. We first stained wild-type and *hcp-1/2(RNAi)* embryos with antibodies against CeMCAK and CeBUB-1. In agreement with an earlier report (Oegema *et al*., 2001), we found that CeBUB-1 localized to wild-type kinetochores during prophase (n = 6), prometaphase (n = 5), metaphase (n = 6; Figure 7A), and mid-anaphase (n = 8; Figure 7A). Also in agreement with previous work, CeMCAK localized in wild-type embryos to centrosomes during prophase (n = 8) and at centrosomes and kinetochores throughout prometaphase (n = 3), metaphase (n = 4; Figure 7A), anaphase (n = 6; Figure 7A), and telophase (n = 4). In *hcp-1/2(RNAi)* embryos, both CeBUB-1 (n = 14) and CeMCAK (n = 22) localized normally to kinetochores during mitosis (Figure 7A), suggesting that HCP-1 is not required for either the stability or the proper localization of these proteins. By contrast, in CeBUB-1–depleted embryos (12/12) and in CeMCAK-depleted embryos (36/37), HCP-1 was either absent or localized diffusely around DNA but apparently not at kinetochores (Figure 7B). Even though HCP-1 localization to kinetochores requires CeBUB-1, depletion of CeBUB-1 and HCP-1/2 results in distinct defects that do not clearly overlap beyond their shared requirement for checkpoint function. In particular, depletion of HCP-1/2 results in more severe spindle defects than does depletion of CeBUB-1. One possible explanation is that HCP-2 might localize to kinetochores independently of CeBUB-1 and HCP-1 and thus fulfill requirements for HCP-1/2 in CeBUB-1–depleted embryos. The lack of an HCP-2 antibody has prevented us from examining this issue further. In summary, HCP-1 localization to chromosomes depends on both CeBUB-1 and CeMCAK but not vice versa (Figure 7C).

DISCUSSION

Mitotic checkpoints are known to delay progression through mitosis in yeast and vertebrate mutants with defective spindles (Gardner and Burke, 2000; Cleveland *et*

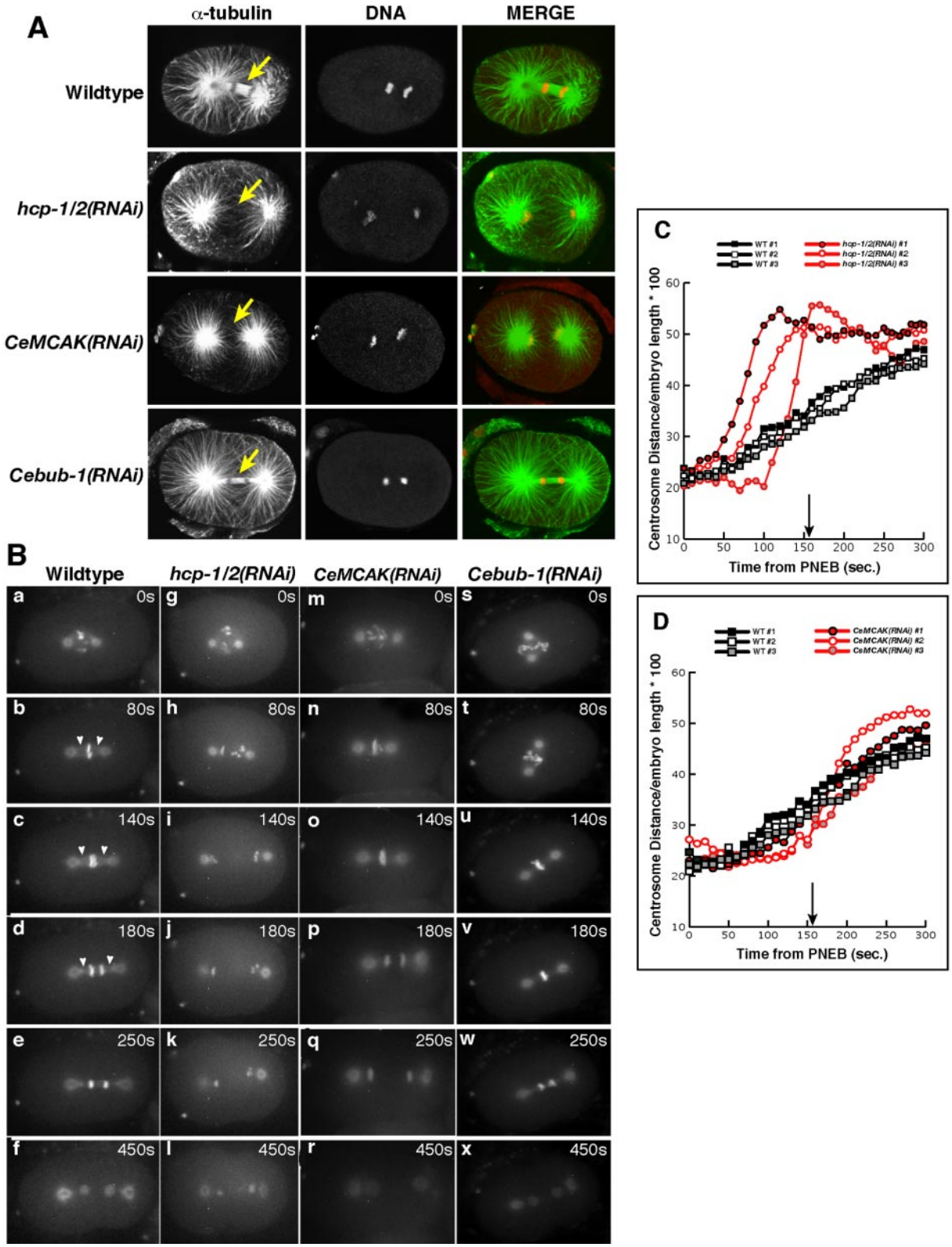

Figure 6. Spindle abnormalities in *hcp-1/2(RNAi)*, *CeMCAK(RNAi)*, and *Cebub-1(RNAi)* mutant embryos. (A) One-cell wild-type, *hcp-1/2(RNAi)*, *CeMCAK(RNAi)*, and *Cebub-1(RNAi)* embryos were fixed and stained to simultaneously visualize DNA (red) and α-tubulin (green). Arrows point to midzone spindle in wild-type and *Cebub-1(RNAi)* embryos, which is absent in *hcp-1/2(RNAi)* and *CeMCAK(RNAi)* embryos. (B) Still images from spinning disk confocal movies of wild-type, *hcp-1/2(RNAi)*, *CeMCAK(RNAi)*, and *Cebub-1(RNAi)* embryos expressing β-tubulin::GFP; histone::GfP constructs. Arrowheads in wild-type images point to spindle microtubule attachments between centrosomes and chromosomes. (C and D) Centrosome separation as a percentage of embryo length plotted for three wild-type (squares) and three *hcp1/2(RNAi)*, (circles) (C) and *CeMCAK(RNAi)*, (circles) (D) embryos. Arrows in both C and D indicate the time of anaphase onset in wild-type embryos.

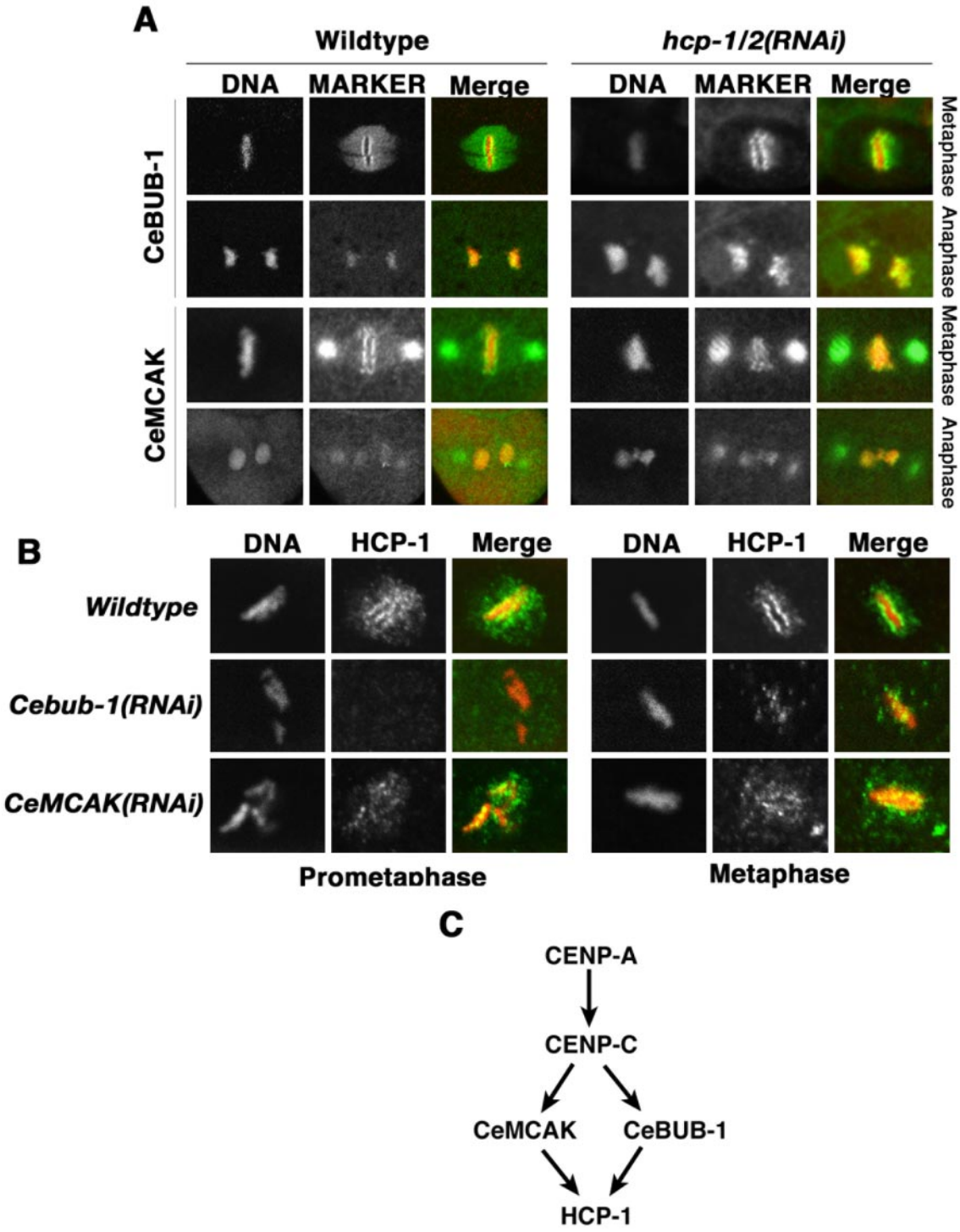

Figure 7. HCP-1 requires CeMCAK and CeBUB-1 for proper localization to kinetochores. (A) Confocal micrographs of metaphase and anaphase wild-type or *hcp1/2(RNAi)* embryos fixed and stain to visualize DNA (TOTO, red) and either CeBUB-1 or CeMCAK (green). (B) Confocal micrographs of wild-type, *Cebub-1(RNAi)* or *CeMCAK(RNAi)* embryos at prometaphase and metaphase fixed and stained with anti HCP-1 antibodies. HCP-1 is not detected at prometaphase and is not targeted to kinetochores at metaphase in *Cebub-1(RNAi)* embryos. Localization of HCP-1 is also disrupted at prometaphase and metaphase in *CeMCAK(RNAi)* embryos. (C) Dependency relationships between kinetochore and spindle checkpoint components position HCP-1 downstream of CeMCAK and CeBUB-1.

al., 2003). We have shown here that a spindle checkpoint in *C. elegans* delays progression through mitosis when spindles are defective in rapidly dividing early embryonic cells. In addition to documenting requirements for known checkpoint proteins, we also have shown that the kinetochore proteins CeCENP-C, CeMCAK and two CENP-F-like proteins called HCP-1/2 are required for spindle checkpoint function.

A Functional Spindle Checkpoint Mechanism in an Early Animal Embryo

We have shown that a spindle assembly checkpoint in early *C. elegans* embryonic cells can delay mitosis both after treatment with nocodazole to destabilize microtubules and in several mutants with defective spindles. Although reproducible, the average duration of the delays is modest compared with those reported for other cell types after exposure to chemicals that stabilize or destabilize microtubules, including PtK1 cells (Waters *et al*., 1998) and sea urchin embryos (Sluder and Begg, 1983). In some cases, such as in HeLa cells, an apparently permanent arrest occurs at the metaphase/anaphase stage (Jordan *et al*., 1996). In *C. elegans*, a cell cycle delay or arrest in response to nocodazole, detected in fixed premeiotic germline cells as an increase in the number of histone H3-positive mitotic cells, was dependent on *mdf-1* and *mdf-2* function (Kitagawa and Rose, 1999). Furthermore, spindle checkpoint function is required for a suspended animation that occurs in response to hypoxia in early *C. elegans* embryos (Nystul *et al*., 2003). Our results suggest that a mitotic checkpoint mechanism functions at least during the first two divisions of the *C. elegans* embryo to produce modest delays in cell cycle progression. Perhaps the modest magnitude of these delays is sufficient to prevent some defects in chromosome segregation, with the duration limited by a need for coordinated cell divisions to properly position descendants during embryogenesis.

In contrast to our findings, studies of early embryonic cell cycles in *Xenopus laevis* have not identified a functional spindle checkpoint, although it is clear that mitotic checkpoint genes act later in embryogenesis and postembryonically (Cleveland *et al*., 2003). The first 12 embryonic cell divisions in *Xenopus* proceed without an effective mitotic checkpoint, because inhibition of spindle assembly does not prevent the regular oscillation of the maturation promoting factor (Gerhart *et al*., 1984). In vitro activation of the spindle checkpoint in early *Xenopus* extracts has been achieved only after adding sperm nuclei to generate a chromosome/cytoplasm ratio comparable with that present at the midblastula transition, when spindle checkpoints normally become active (Minshull *et al*., 1994).

The apparent absence of a spindle checkpoint in early *Xenopus* embryos has led to suggestions that the rapid early embryonic cell cycles observed in some organisms may be devoid of mitotic checkpoint regulation (Murray and Hunt, 1997; Hartwell and Weinert, 1989). In *Drosophila melanogaster*, mutational inactivation of the spindle checkpoint genes *bub1*, *Rod*, and *Zw10* result in an accelerated exit from metaphase and chromosome segregation defects in larval brain cells and neuroblasts with defective mitotic spindles, but earlier embryonic defects have not been reported (Basu *et al*., 1999; Basto *et al*., 2000). However, maternal expression of these genes could mask earlier requirements during embryogenesis, and treatment of early *Drosophila* embryos with nocodazole does result in mitotic delays (Yu *et al*., 1998). Evidence for a functional spindle checkpoint during meiosis in mouse oocytes suggests that the checkpoint machinery is present in early mammalian embryos (Wassmann *et al*., 2003). Thus, it seems likely that other early embryos will be found to use, perhaps to varying degrees, a spindle checkpoint during early embryonic cell cycles.

One difference between *C. elegans* and most other eukaryotic organisms is that *C. elegans* chromosomes are holocentric, not centromeric (Pimpinelli and Goday, 1989; reviewed in Maddox *et al*., 2004). Microtubules attach along the entire length of holocentric chromosomes, and all *C. elegans* kinetochore proteins studied to date localize along the entire length of mitotic chromosomes, including the proteins that we report in this study to be involved in spindle checkpoint function (Figure 7, A and B). How the spindle checkpoint can monitor many attachment sites in holocentric chromosomes and how mechanistically distinct might be the monitoring mechanisms for monocentric chromosomes remain unknown.

Although we have documented mitotic delays in several different mutants, mitotic delays have not been observed in some *C. elegans* mutants with severe spindle assembly defects in early embryonic cells. For example, embryonic cells depleted of AIR-1, an aurora-A kinase required for centrosome maturation, produce a very small but still bipolar spindle with reduced centrosomes, yet the timing of progression through metaphase and anaphase was normal (Schumacher *et al*., 1998; Hannak *et al*., 2001). Similarly, we have found that embryos lacking SPD-5, a coiled-coil centrosomal protein required for centrosome maturation and assembly of a mitotic spindle (Hamill *et al*., 2002), exhibit normal mitotic timing (our unpublished data). Further investigation of spindle and kinetochore assembly in these exceptional mutants should provide further insights into the assembly of a functional spindle checkpoint.

Differential Control of Cell Division Timing in Early Embryos

In contrast to *Xenopus* and *Drosophila*, cell divisions in the early *C. elegans* embryo are asynchronous (Sulston *et al*., 1983). These early divisions seem to consist entirely of S phase and mitosis, with differences in division timing being due to different rates of DNA replication during S phase (Edgar and McGhee, 1988). The differences in timing were recently shown to depend in part on the widely conserved DNA replication checkpoint, which can delay progression through S phase in response to defects in DNA replication in early embryonic cells (Brauchle *et al*., 2003). Similarly in *Drosophila*, a DNA replication/damage checkpoint regulated by *grapes* and Mei-41/ATM has been found to operate during late syncytial embryonic divisions to ensure proper DNA replication before entry into mitosis (Fogarty *et al*., 1997; Sibon *et al*., 1999). In contrast to S phase, the duration of mitosis is roughly constant in different early *C. elegans* embryonic cells (Edgar and McGhee, 1988; Encalada *et al*., 2000), suggesting that the differential control of mitotic progression by the spindle checkpoint does not contribute to the asynchrony of early embryonic cell cycles.

Kinetochore Proteins and Spindle Checkpoint Function

The restoration of normal mitotic timing in embryos with defective spindles, after depletion of MDF-1, MDF-2, CeCENP-C, CeMCAK, HCP-1/2, and perhaps CeBUB-1, indicates that these proteins are involved in mitotic checkpoint activity in the early *C. elegans* embryo. This checkpoint function could be direct, despite other potential roles for some of these proteins in kinetochore and/or spindle midzone structure. For example, the poleward movement of centrosomes and chromosomes during anaphase in *CeMCAK(RNAi)* and *hcp-1/2(RNAi)* embryos suggests that kinetochore-microtubule interactions were not entirely absent and thus that these genes are not entirely required for kinetochore function (although this residual kinetochore function might be due to incomplete knockdown of CeMCAK and HCP-1/2 by RNAi). Furthermore, both CeMCAK and HCP-1 assemble onto kinetochores downstream of CENP-A and CENP-C, two core structural kinetochore proteins (Moore *et al*., 1999; Oegema *et al*., 2001). Thus, CeMCAK and HCP-1/2 do not seem to disrupt kineto-

chore structure generally and could be involved more directly in checkpoint assembly or function. Indeed, the precocious anaphase observed in *hcp-1/2(RNAi)* embryos is characteristic of other spindle checkpoint proteins (Gorbsky *et al*., 1998; Canman *et al*., 2002) and is consistent with the role of *hcp-1/2* in checkpoint function.

However, we cannot rule out the possibility that these checkpoint requirements could be largely indirect, reflecting more general structural roles in kinetochore assembly. Indeed, it has been shown previously that CeCENP-C is necessary for kinetochore assembly in early embryonic cells (Oegema *et al*., 2001), and the lack of spindle checkpoint delays in *CeCENP-C(RNAi)* mutants could be attributed to the absence of kinetochores.

Kinetochore Proteins Function in a Complex Network of Spindle Midzone Formation and Spindle Checkpoint Pathways

Our analysis of the functional requirements for CeMCAK, HCP-1/2, and CeBUB-1 suggests that in addition to having spindle checkpoint roles, CeMCAK and HCP-1/2 also function in spindle midzone formation and spindle checkpoint pathways. CeBUB-1 might be required more specifically for proper mitotic checkpoint activity, although it also is required for chromosome segregation. Thus, our data together with data from previous studies define at least four overlapping classes of kinetochore proteins: core kinetochore components (CeCENP-A and CeCENP-C), spindle midzone formation factors (CeMCAK and HCP-1/2), chromosome segregation factors (CeMCAK, HCP-1/2, and CeBUB-1), and spindle checkpoint signaling proteins (MDF-1, MDF-2, CeCENP-C, CeMCAK, CeBUB-1, and HCP-1/2).

Although the requirements for these kinetochore proteins are complex and overlapping, we can detect some hierarchical relationships, or pathways. For example, embryos depleted of CeMCAK or CeBUB-1 fail to localize HCP-1 to kinetochores, whereas CeMCAK and CeBUB-1 localize to kinetochores in the absence of HCP-1/2, suggesting that both CeMCAK and CeBUB-1 act upstream of HCP-1/2 (Figure 7C). These results are in agreement with labeling experiments in U2OS osteosarcoma cells and HeLa cells, in which microinjection of anti-hBUB-1 and anti-hCENP-F antibodies suggest that hBUB-1 assembles onto kinetochores before hCENP-F, and with yeast two hybrid data suggesting that CENP-F binds Bub-1 (Jablonski *et al*., 1998). However, it is not clear why, in spite of both CeBUB-1 and CeMCAK being required for HCP-1 localization, *hcp-1/2(RNAi)* embryos seem to have a more severe phenotype than either CeMCAK(RNAi) or especially *Cebub-1(RNAi)* embryos. Moreover, *Cebub-1(RNAi); CeMCAK(RNAi*) double mutant embryos do not exhibit the severe phenotype of *hcp-1/2(RNAi)* embryos (our unpublished data). Thus, other proteins besides CeMCAK and CeBUB-1 might regulate HCP-1/2 function. The localization of HCP-2 is not known, and it would be interesting to learn whether HCP-2 is at kinetochores and functional in the absence of CeBUB-1 or CeMCAK. Although apparently redundant in function, HCP-1 and HCP-2 share only 54% similarity and could have different requirements for their localization to kinetochores.

CeMCAK, CeBUB-1, and HCP-1 have all been positioned downstream of two core kinetochore proteins, CeCENP-A and CeCENP-C (Moore *et al*., 1999; Oegema *et al*., 2001). Interestingly, the phenotypes of *hcp-1/2(RNAi)* and *CeMCAK(RNAi)* embryos differ substantially from the phenotypes of embryos depleted of CeCENP-A and CeCENP-C in that chromosomes do not exhibit poleward movement in *CeCENP-A(RNAi)* and *CeCENP-C(RNAi)* embryos (Oegema *et al*., 2001). The less general requirements for some kinetochore proteins further implies a hierarchy in functional assembly. However, the interplay and coordination between kinetochore and spindle checkpoint proteins seem complex and may not be easily explained by simple linear pathways. Moreover, until definitive null phenotypes have been defined, it may prove difficult to distinguish the requirements for different loci based only on RNAi-mediated depletion of proteins.

Is CeMCAK a Bridge between Kinetochores and Microtubules?

We think it is particularly interesting to consider a direct role for CeMCAK in checkpoint function. One possibility is that CeMCAK might link kinetochores to spindle microtubules, as proposed for the kinetochore kinesin CENP-E in vertebrate cells (Abrieu *et al*., 2000). The motor activity of CENP-E is thought to generate tension at the kinetochore/microtubule interface upon capture of microtubules, while also conveying checkpoint signaling activities to other checkpoint proteins (Abrieu *et al*., 2000). BLAST searches indicate that a CENP-E sequence homolog does not exist in *C. elegans*, and a functional homolog has not been identified. Three observations support the possibility that CeMCAK might act like CENP-E to influence checkpoint signaling. First, in contrast to the vertebrate MCAK family members that localize to inner centromeres between paired sister chromatid kinetochores (Wordeman and Mitchison, 1995; Walczak *et al*., 1996), CeMCAK localizes to outer kinetochores in *C. elegans* (Oegema *et al*., 2001). Moreover, whereas vertebrate MCAK colocalizes with Aurora B, an established inner centromere protein (Adams *et al*., 2001; Shannon and Salmon, 2002; Cleveland *et al*., 2003), CeMCAK localizes to kinetochores independent of the inner centromere proteins CeINCENP and AIR-2/CeAurora B (Oegema *et al*., 2001). Thus, CeMCAK is positioned to interact with kinetochore microtubules and influence checkpoint function, in contrast to some of its vertebrate relatives. Second, studies in *Xenopus* extracts have shown that XMCAK promotes microtubule depolymerization during mitotic spindle assembly (Walczak *et al*., 1996), and depolymerization at microtubule minus-ends can generate forces to pull chromosomes in the absence of ATP-dependent forces (Coue *et al*., 1991). Thus, CeMCAK may have activities appropriate for generating force at kinetochores. Finally, CeMCAK is required for HCP-1 localization to kinetochores, which we show, together with CeBUB-1, is required for checkpoint function. Thus, CeMCAK is closely linked to spindle checkpoint proteins and could transmit the contact/tension generated at the microtubule/kinetochore interface to mitotic checkpoint proteins. If, as these observations suggest, CeMCAK does function like vertebrate CENP-E, then animal cells apparently have evolved multiple solutions to the assembly of functional kinetochore and spindle checkpoint complexes during mitosis.

ACKNOWLEDGMENTS

We thank Dan Burke, Julie Canman, Chris Doe, Judith Eisen, Tom Hays, and Marc Meneghini for helpful comments on the manuscript. We thank Yuji Kohara for providing cDNA clones, the *Caenorhabditis elegans* Genetics Center (funded by the National Institutes of Health) for strains, Joe Christison for preliminary studies of the *hcp-1/2(RNAi)* phenotype, and members of the Bowerman laboratory for helpful discussions. We are grateful to Karen Oegema for anti-CeBUB-1 and anti-CeMCAK antibodies and to Mark Roth for the anti-HCP-1 antibody. This work was supported by National Institutes of Health training grants (to S. E. and J. W.), by the American Cancer Society (to R. L.), and by National Institutes of Health research grant GM-49869 (to B. B.).

REFERENCES

Abrieu, A., Kahana, J. A., Wood, K. W., and Cleveland, D. W. (2000). CENP-E as an essential component of the mitotic checkpoint in vitro. Cell *102*, 817–826.

Adams, R. R., Carmena, M., and Earnshaw, W. C. (2001). Chromosomal passengers and the (aurora) ABCs of mitosis. Trends Cell Biol. *11*, 49–54.

Basto, R., Gomes, R., and Karess, R. E. (2000). Rough deal and Zw10 are required for the metaphase checkpoint in *Drosophila*. Nat. Cell Biol. 2, 939–943.

Basu, J., Bousbaa, H., Logarinho, E., Li, Z., Williams, B. C., Lopes, C., Sunkel, C. E., and Goldberg, M. L. (1999). Mutations in the essential spindle checkpoint gene bub1 cause chromosome missegregation and fail to block apoptosis in *Drosophila*. J. Cell Biol. *146*, 13–28.

Brauchle, M., Baumer, K., and Gonczy, P. (2003). Differential activation of the DNA replication checkpoint contributes to asynchrony of cell division in *C. elegans* embryos. Curr. Biol. *13*, 819–827.

Brenner, S. (1974). The genetics of *Caenorhabditis elegans*. Genetics *77*, 71–94.

Buchwitz, B. J., Ahmad, K., Moore, L. L., Roth, M. B., and Henikoff, S. (1999). A histone-H3-like protein in *C. elegans*. Nature *401*, 547–548.

Canman, J. C., Salmon, E. D., and Fang, G. (2002). Inducing precocious anaphase in cultured mammalian cells. Cell Motil. Cytoskeleton *52*, 61–65.

Chan, G. K., Schaar, B. T., and Yen, T. J. (1998). Characterization of the kinetochore binding domain of CENP-E reveals interactions with the kinetochore proteins CENP-F and hBUBR1. J. Cell Biol. *143*, 49–63.

Cleveland, D. W., Mao, Y., and Sullivan, K. F. (2003). Centromeres and kinetochores: from epigenetics to mitotic checkpoint signaling. Cell *112*, 407–421.

Coue, M., Lombillo, V. A., and McIntosh, J. R. (1991). Microtubule depolymerization promotes particle and chromosome movement in vitro. J. Cell Biol. *112*, 1165–1175.

Desai, A., Rybina, S., Muller-Reichert, T., Shevchenko, A., Hyman, A., and Oegema, K. (2003). KNL-1 directs assembly of the microtubule-binding interface of the kinetochore in *C. elegans*. Genes Dev. *17*, 2421–2435.

Eaker, S., Pyle, A., Cobb, J., and Handel, M. A. (2001). Evidence for meiotic spindle checkpoint from analysis of spermatocytes from Robertsonian-chromosome heterozygous mice. J. Cell Sci. *114*, 2953–2965.

Edgar, L. G., and McGhee, J. D. (1988). DNA synthesis and the control of embryonic gene expression in *C. elegans*. Cell *53*, 589–599.

Encalada, S. E., Martin, P. R., Phillips, J. B., Lyczak, R., Hamill, D. R., Swan, K. A., and Bowerman, B. (2000). DNA replication defects delay cell division and disrupt cell polarity in early *Caenorhabditis elegans* embryos. Dev. Biol. *228*, 225–238.

Foe, V. E., and Alberts, B. M. (1983). Studies of nuclear and cytoplasmic behaviour during the five mitotic cycles that precede gastrulation in *Drosophila* embryogenesis. J. Cell Sci. *61*, 31–70.

Fogarty, P., Campbell, S. D., Abu-Shumays, R., Phalle, B. S., Yu, K. R., Uy, G. L., Goldberg, M. L., and Sullivan, W. (1997). The *Drosophila grapes* gene is related to checkpoint gene chk1/rad27 and is required for late syncytial division fidelity. Curr. Biol. *7*, 418–426.

Gardner, R. D., and Burke, D. J. (2000). The spindle checkpoint: two transitions, two pathways. Trends Cell Biol. *10*, 154–158.

Gerhart, J., Wu, M., and Kirschner, M. (1984). Cell cycle dynamics of an M-phase-specific cytoplasmic factor in *Xenopus laevis* oocytes and eggs. J. Cell Biol. *98*, 1247–1255.

Gonczy, P., Pichler, S., Kirkham, M., and Hyman, A. A. (1999). Cytoplasmic dynein is required for distinct aspects of MTOC positioning, including centrosome separation, in the one cell stage *Caenorhabditis elegans* embryo. J. Cell Biol. *147*, 135–150.

Gorbsky, G. J., Chen, R. H., and Murray, A. W. (1998). Microinjection of antibody to Mad2 protein into mammalian cells in mitosis induces premature anaphase. J. Cell Biol. *141*, 1193–1205.

Grill, S. W., Gonczy, P., Stelzer, E. H., and Hyman, A. A. (2001). Polarity controls forces governing asymmetric spindle positioning in the *Caenorhabditis elegans* embryo. Nature *409*, 630–633.

Hamill, D. R., Severson, A. F., Carter, J. C., and Bowerman, B. (2002). Centrosome maturation and mitotic spindle assembly in *C. elegans* require SPD-5, a protein with multiple coiled-coil domains. Dev. Cell *3*, 673–684.

Hannak, E., Kirkham, M., Hyman, A. A., and Oegema, K. (2001). Aurora-A kinase is required for centrosome maturation in *Caenorhabditis elegans*. J. Cell Biol. *155*, 1109–1116.

Hardwick, K. G., and Murray, A. W. (1995). Mad1p, a phosphoprotein component of the spindle assembly checkpoint in budding yeast. J. Cell Biol. *131*, 709–720.

Hardwick, K. G., Weiss, E., Luca, F. C., Winey, M., and Murray, A. W. (1996). Activation of the budding yeast spindle assembly checkpoint without mitotic spindle disruption. Science *273*, 953–956.

Hartwell, L. H., and Weinert, T. A. (1989). Checkpoints: controls that ensure the order of cell cycle events. Science *246*, 629–634.

Hartwell, L. H., and Kastan, M. B. (1994). Cell cycle control and cancer. Science *266*, 1821–1828.

Hoyt, M. A., Totis, L., and Roberts, B. T. (1991). *S. cerevisiae* genes required for cell cycle arrest in response to loss of microtubule function. Cell *66*, 507–517.

Hwang, L. H., Lau, L. F., Smith, D. L., Mistrot, C. A., Hardwick, K. G., Hwang, E. S., Amon, A., and Murray, A. W. (1998). Budding yeast Cdc *20*, a target of the spindle checkpoint. Science *279*, 1041–1044.

Hyman, A. A., and White, J. G. (1987). Determination of cell division axes in the early embryogenesis of *Caenorhabditis elegans*. J. Cell Biol. *105*, 2123–2135.

Jablonski, S. A., Chan, G. K., Cooke, C. A., Earnshaw, W. C., and Yen, T. J. (1998). The hBUB1 and hBUBR1 kinases sequentially assemble onto kinetochores during prophase with hBUBR1 concentrating at the kinetochore plates in mitosis. Chromosoma *107*, 386–396.

Jordan, M. A., Wendell, K., Gardiner, S., Derry, W. B., Copp, H., and Wilson, L. (1996). Mitotic block induced in HeLa cells by low concentrations of paclitaxel (Taxol) results in abnormal mitotic exit and apoptotic cell death. Cancer Res. *56*, 816–825.

Kitagawa, R., and Rose, A. M. (1999). Components of the spindle-assembly checkpoint are essential in *Caenorhabditis elegans*. Nat. Cell Biol. *1*, 514–521.

Kurz, T., Pintard, L., Willis, J. H., Hamill, D. R., Gonczy, P., Peter, M., and Bowerman, B. (2002). Cytoskeletal regulation by the Nedd8 ubiquitin-like protein modification pathway. Science *295*, 1294–1298.

Li, R., and Murray, A. W. (1991). Feedback control of mitosis in budding yeast. Cell *66*, 519–531.

Liao, H., Winkfein, R. J., Mack, G., Rattner, J. B., and Yen, T. J. (1995). CENP-F is a protein of the nuclear matrix that assembles onto kinetochores at late G2 and is rapidly degraded after mitosis. J. Cell Biol. *130*, 507–518.

Maddox, P. S., Oegema, K., Desai, A., and Cheeseman, I. M. (2004). "Holo"er than thou: chromosome segregation and kinetochore function in *C. elegans*. Chromosome Res. *12*, 641–653.

Matthews, L. R., Carter, P., Thierry-Mieg, D., and Kemphues, K. (1998). ZYG-9, a *Caenorhabditis elegans* protein required for microtubule organization and function, is a component of meiotic and mitotic spindle poles. J. Cell Biol. *141*, 1159–1168.

McIntosh, J. R., Grishchuk, E. L., and West, R. R. (2002). Chromosome–microtubule interactions during mitosis. Annu. Rev. Cell Dev. Biol. *18*, 193–219.

Minshull, J., Sun, H., Tonks, N. K., and Murray, A. W. (1994). A MAP kinase-dependent spindle assembly checkpoint in *Xenopus* egg extracts. Cell *79*, 475–486.

Moore, L. L., Morrison, M., and Roth, M. B. (1999). HCP-1, a protein involved in chromosome segregation, is localized to the centromere of mitotic chromosomes in *Caenorhabditis elegans*. J. Cell Biol. *147*, 471–480.

Moore, L. L., and Roth, M. B. (2001). HCP-4, a CENP-C-like protein in *Caenorhabditis elegans*, is required for resolution of sister centromeres. J. Cell Biol. *153*, 1199–1208.

Murray, A. W., and Hunt, T. (1997). The Cell Cycle: An Introduction, Oxford, NY: Oxford University Press.

Nystul, T. G., Goldmark, J. P., Padilla, P. A., and Roth, M. B. (2003). Suspended animation in *C. elegans* requires the spindle checkpoint. Science *302*, 1038–1041.

Oegema, K., Desai, A., Rybina, S., Kirkham, M., and Hyman, A. A. (2001). Functional analysis of kinetochore assembly in *Caenorhabditis elegans*. J. Cell Biol. *153*, 1209–1226.

Pangilinan, F., and Spencer, F. (1996). Abnormal kinetochore structure activates the spindle assembly checkpoint in budding yeast. Mol. Biol. Cell *7*, 1195–1208.

Pimpinelli, S., and Goday, C. (1989). Unusual kinetochores and chromatin diminution in *Parascaris*. Trends Genet. *5*, 310–315.

Praitis, V., Casey, E., Collar, D., and Austin, J. (2001). Creation of low-copy integrated transgenic lines in *Caenorhabditis elegans*. Genetics *157*, 1217–1226.

Raich, W. B., Moran, A. N., Rothman, J. H., and Hardin, J. (1998). Cytokinesis and midzone microtubule organization in *Caenorhabditis elegans* require the kinesin-like protein ZEN-4. Mol. Biol. Cell *9*, 2037–2049.

Schumacher, J. M., Ashcroft, N., Donovan, P. J., and Golden, A. (1998). A highly conserved centrosomal kinase, AIR-1, is required for accurate cell cycle progression and segregation of developmental factors in *Caenorhabditis elegans* embryos. Development *125*, 4391–4402.

Salina, D., Bodoor, K., Eckley, D. M., Schroer, T. A., Rattner, J. B., and Burke, B. (2002). Cytoplasmic dynein as a facilitator of nuclear envelope breakdown. Cell *108*, 97–107.

Shannon, K. B., and Salmon, E. D. (2002). Chromosome dynamics: new light on Aurora B kinase function. Curr. Biol. *12*, R458–R460.

Sibon, O. C., Laurencon, A., Hawley, R., and Theurkauf, W. E. (1999). The *Drosophila* ATM homologue Mei-41 has an essential checkpoint function at the midblastula transition. Curr. Biol. *9*, 302–312.

Skibbens, R. V., and Hieter, P. (1998). Kinetochores and the checkpoint mechanism that monitors for defects in the chromosome segregation machinery. Annu. Rev. Genet. *32*, 307–337.

Skop, A. R., and White, J. G. (1998). The dynactin complex is required for cleavage plane specification in early *Caenorhabditis elegans* embryos. Curr. Biol. *8*, 1110–1116.

Sluder, G., and Begg, D. A. (1983). Control mechanisms of the cell cycle: role of the spatial arrangement of spindle components in the timing of mitotic events. J. Cell Biol. *97*, 877–886.

Strome, S., Powers, J., Dunn, M., Reese, K., Malone, C. J., White, J., Seydoux, G., and Saxton, W. (2001). Spindle dynamics and the role of gamma-tubulin in early *Caenorhabditis elegans* embryos. Mol. Biol. Cell *12*, 1751–1764.

Strome, S., and Wood, W. B. (1983). Generation of asymmetry and segregation of germ-line granules in early *C. elegans* embryos. Cell *35*, 15–25.

Sullivan, W., Daily, D. R., Fogarty, P., Yook, K. J., and Pimpinelli, S. (1993). Delays in anaphase initiation occur in individual nuclei of the syncytial *Drosophila* embryo. Mol. Biol. Cell *4*, 885–896.

Sulston, J. E., Schierenberg, E., White, J. G., and Thomson, J. N. (1983). The embryonic cell lineage of the nematode *Caenorhabditis elegans*. Dev. Biol. *100*, 64–119.

Sweeney, H. L., and Holzbaur, E. L. (1996). Mutational analysis of motor proteins. Annu. Rev. Physiol. *58*, 751–792.

Walczak, C. E., Mitchison, T. J., and Desai, A. (1996). XKCM *1*, a *Xenopus* kinesin-related protein that regulates microtubule dynamics during mitotic spindle assembly. Cell *84*, 37–47.

Wang, Y., and Burke, D. J. (1995). Checkpoint genes required to delay cell division in response to nocodazole respond to impaired kinetochore function in the yeast *Saccharomyces cerevisiae*. Mol. Cell. Biol. *15*, 6838–6844.

Wassmann, K., Niault, T., and Maro, B. (2003). Metaphase I arrest upon activation of the Mad2-dependent spindle checkpoint in mouse oocytes. Curr. Biol. *13*, 1596–1608.

Waters, J. C., Chen, R. H., Murray, A. W., and Salmon, E. D. (1998). Localization of Mad2 to kinetochores depends on microtubule attachment, not tension. J. Cell Biol. *141*, 1181–1191.

Weaver, B. A., Bonday, Z. Q., Putkey, F. R., Kops, G. J., Silk, A. D., and Cleveland, D. W. (2003). Centromere-associated protein-E is essential for the mammalian mitotic checkpoint to prevent aneuploidy due to single chromosome loss. J. Cell Biol. *162*, 551–563.

Wordeman, L., and Mitchison, T. J. (1995). Identification and partial characterization of mitotic centromere-associated kinesin, a kinesin-related protein that associates with centromeres during mitosis. J. Cell Biol. *128*, 95–104.

Yu, K. R., Duronio, R. J., and Sullivan, W. (1998). Cell cycle checkpoints: safe passage through mitosis. In: Mechanisms of Cell Division: Frontiers in Biology. ed. S. Endow and D. Glover, New York: Oxford University Press, 1–41.

Zalokar, M. (1976). Autoradiographic study of protein and RNA formation during early development of *Drosophila* eggs. Dev. Biol. *49*, 425–437.

Zhu, X., Chang, K. H., He, D., Mancini, M. A., Brinkley, W. R., and Lee, W. H. (1995). The C terminus of mitosin is essential for its nuclear localization, centromere/kinetochore targeting, and dimerization. J. Biol. Chem. *270*, 19545–19550.